Gene 668 (2018) 87–96

Contents lists available at ScienceDirect

Gene

journal homepage: www.elsevier.com/locate/gene

Research paper

Molecular characterization of physis tissue by RNA sequencing☆

Christopher R. Paradise[a,b,c], Catalina Galeano-Garces[b,d], Daniela Galeano-Garces[b], Amel Dudakovic[b], Todd A. Milbrandt[b], Daniel B.F. Saris[a,b,d,e], Aaron J. Krych[b,f], Marcel Karperien[d], Gabriel B. Ferguson[g], Denis Evseenko[g], Scott M. Riester[b], Andre J. van Wijnen[a,b,h,*], A. Noelle Larson[b,*]

[a] Center for Regenerative Medicine, Mayo Clinic, Rochester, MN, USA
[b] Department of Orthopedic Surgery, Mayo Clinic, Rochester, MN, USA
[c] Mayo Clinic Graduate School of Biomedical Sciences, Mayo Clinic, Rochester, MN, USA
[d] Department of Developmental BioEngineering, University of Twente, Enschede, Netherlands
[e] Department of Orthopaedics, University Medical Center Utrecht, Utrecht University, Utrecht, Netherlands
[f] Department of Sports Medicine, Mayo Clinic, Rochester, MN, USA
[g] Department of Orthopaedic Surgery, University of Southern California (USC), Los Angeles, CA, USA
[h] Department of Biochemistry and Molecular Biology, Mayo Clinic, Rochester, MN, USA

ARTICLE INFO

Keywords:
Physis
Growth plate
RNA sequencing
Bone
Cartilage

ABSTRACT

The physis is a well-established and anatomically distinct cartilaginous structure that is crucial for normal long-bone development and growth. Abnormalities in physis function are linked to growth plate disorders and other pediatric musculoskeletal diseases. Understanding the molecular pathways operative in the physis may permit development of regenerative therapies to complement surgically-based procedures that are the current standard of care for growth plate disorders. Here, we performed next generation RNA sequencing on mRNA isolated from human physis and other skeletal tissues (e.g., articular cartilage and bone; n = 7 for each tissue).

We observed statistically significant enrichment of gene sets in the physis when compared to the other musculoskeletal tissues. Further analysis of these upregulated genes identified physis-specific networks of extracellular matrix proteins including collagens (COL2A1, COL6A1, COL9A1, COL14A1, COL16A1) and matrilins (MATN1, MATN2, MATN3), and signaling proteins in the WNT pathway (WNT10B, FZD1, FZD10, DKK2) or the FGF pathway (FGF10, FGFR4). Our results provide further insight into the gene expression networks that contribute to the physis' unique structural composition and regulatory signaling networks. Physis-specific expression profiles may guide ongoing initiatives in tissue engineering and cell-based therapies for treatment of growth plate disorders and growth modulation therapies. Furthermore, our findings provide new leads for therapeutic drug discovery that would permit future intervention through pharmacological rather than surgical strategies.

1. Introduction

Leg length discrepancy and angular limb deformities are common pediatric disorders that result in pain, limp and potential lifelong disability. To treat growth plate or physeal disorders, children frequently require complex surgical reconstructions to alleviate symptoms and restore functional capacity. Current treatments include manipulation of the growth plate by surgically tethering or ablating the physis, resection of damaged portions of the growth plate to restore growth, and limb lengthening procedures using distraction osteogenesis (Sanders et al.

Abbreviations: NCATS, National Center for Advancing Translational Sciences; NIH, National Institutes of Health; COL2A1, collagen Type II alpha 1 chain; COL6A1, collagen type VI alpha 1 chain; COL9A1, collagen type IX alpha 1 chain; COL9A2, collagen type IX alpha 2 chain; COL9A3, collagen type IX alpha 3 chain; COL11A2, collagen type XI alpha 2 chain; COL14A1, collagen type XIV alpha 1 chain; COL16A1, collagen type XVI alpha 1 chain; MATN1, Matrilin 1; MATN2, Matrilin 2; MATN3, Matrilin 3; WNT10B, Wnt Family Member 10B; FZD1, frizzled class receptor 1; FZD2, frizzled class receptor 2; FZD10, frizzled class receptor 10; DKK1, Dickkopf WNT signaling pathway inhibitor 1; DKK2, Dickkopf WNT signaling pathway inhibitor 2; FGF, fibroblast growth factor; FGF10, fibroblast growth factor 10; FGF18, fibroblast growth factor 18; FGFR4, fibroblast growth factor receptor 4; RT-qPCR, real-time quantitative polymerase chain reaction; RNA-seq, mRNA sequencing; IRB, institutional review board; SRA, Sequence Read Archive; RIN, RNA Integrity Number; RPKM, reads per kilobasepair per million mapped reads; IHC, immunohistochemistry; BSA, bovine serum albumin; DAB, 3,3′-diaminobenzidine; PCA, principal component analysis; GO, gene ontology; EDS, Ehlers-Danlos Syndrome; ANOVA, analysis of variance; HBB, hemoglobin β

☆ Institution where reported work was done: Mayo Clinic, Rochester, MN, USA.

* Corresponding authors at: Mayo Clinic, 200 First Street SW, Rochester, MN 55905, USA.
E-mail addresses: vanWijnen.Andre@mayo.edu (A.J. van Wijnen), Larson.Noelle@mayo.edu (A. Noelle Larson).

https://doi.org/10.1016/j.gene.2018.05.034
Received 11 May 2018; Accepted 11 May 2018
Available online 25 May 2018
0378-1119/

2007; Stevens 2007; Black et al. 2015; Clark et al. 2015). Although deformities can be corrected using these techniques, they are not always effective and are associated with significant complications such as infection, nerve injury, fracture, and morbidity (Hantes et al. 2001; Launay et al. 2013). Novel strategies such as administration of local pharmacologic agents aimed at selectively enhancing or inhibiting the growth plate function have the potential to improve the clinical outcomes over current treatments by avoiding the pain and morbidity associated with complex surgical reconstructions.

The physis is a unique cartilaginous structure that is responsible for the longitudinal growth of long bones via the process of endochondral ossification (Kronenberg 2003). As a transition zone between resting chondrocytes and newly calcified bone matrix, the physis is comprised of several distinct layers (Marino 2011). Briefly, the reserve or germinal zone contains chondrocyte progenitor cells and resting chondrocytes. This zone is adjacent to the zone of proliferation where chondrocytes multiply and form the classic columnar arrangement before entering the zone of hypertrophy. At this stage, chondrocytes increase in size and reach a terminally differentiated state culminating in cell apoptosis. Osteoblasts fill this void and begin to calcify the extracellular matrix to form the zone of ossification. Longitudinal growth of long bones is mediated by the proliferation of resting chondrocytes and their subsequent hypertrophy (Andrade et al. 2010; Lui et al. 2010). This transition is associated with an increase in extracellular matrix production controlled by a complex regulatory network (Myllyharju 2014). Thus, the growth plate serves as a dynamic transitional tissue between resting chondrocytes and newly formed cortical bone.

Better understanding of the gene expression profile and signaling patterns within the physis may elucidate novel regulatory pathways involved in physis maturation and long-bone development. Insight gained from such an analysis can be leveraged for tissue engineering strategies and/or identification of drug targets for therapeutics aimed to modulate growth plate function. Previous studies from our group and others have demonstrated the utility of mRNA analysis (i.e. RT-qPCR and/or RNA-sequencing) as a means to identify key regulatory gene networks within specific musculoskeletal tissue types or disease states (Lewallen et al. 2016; Lin et al. 2016; Galeano-Garces et al. 2017; Riester et al. 2017). Thus, we sought to identify differentially expressed mRNA transcripts in the physis compared to other musculoskeletal tissues. We provide a detailed comparative analysis of RNA sequencing data derived from physis tissue compared to bone, articular cartilage, and muscle. Further analysis of these differentially expressed genes reveals structural components and signaling pathways distinct to the physis.

2. Methods

2.1. RNA extraction from tissues

Tissue specimens were collected from patients undergoing tissue removal as part of planned surgical procedures (Supplemental Table 1). Each sample was obtained from a different patient with the exception of one matched cartilage and bone sample and another matched pair of physis samples as indicated in the supplementary table. The specimens used in this investigation were collected under institutional review board (IRB) approved protocols (IRB# 13-005403 and 13-005619). Written informed consent was obtained for all biospecimens that were collected. Expression data for two of the samples included in the muscle group were obtained from the Sequence Read Archive (SRA) database (accession numbers SRR1424734 and SRR1424735) (Lindholm et al. 2014).

At the time of surgical harvest, tissues were snap frozen in liquid nitrogen and stored at −80 °C. For bone, articular cartilage, and muscle, frozen tissue biopsies were ground into a powder using a mortar and pestle and homogenized in Qiazol reagent (Qiagen, Hilden, Germany). Total RNA was extracted from research biopsies using the RNeasy minikit (Qiagen, Hilden, Germany) and quantified using the NanoDrop 2000 spectrophotometer (Thermo Fischer Scientific, Wilmington, Delaware). For growth plate specimens, RNA was isolated from the frozen biopsies using AnaPrep Total RNA Extraction Kit (Biochain, Newark, CA) and quantified using the NanoDrop 2000 spectrophotometer (Thermo Fischer Scientific, Wilmington, Delaware). For samples selected for next generation sequencing, RNA integrity was assessed using the Agilent Bioanalyzer DNA 1000 chip (Invitrogen, Carlsbad, CA). Only samples with an RNA Integrity Number (RIN) and DV_{200} score greater than our Sequencing Core's minimum cutoff (RIN > 6 and DV_{200} > 50%) were used for sequencing.

2.2. Next generation mRNA sequencing

RNA sequencing and subsequent bioinformatic analysis were performed in collaboration with the Mayo Clinic RNA sequencing and bioinformatics cores as previously described (Dudakovic et al. 2014; Kalari et al. 2014). In brief, library preparation was performed using the TruSeq RNA library preparation kit (Illumina, San Diego, CA). Polyadenylated mRNAs were selected using oligo dT magnetic beads. TruSeq Kits were used for indexing to permit multiplex sample loading on the flow cells. Paired-end sequencing reads were generated on the Illumina HiSeq 2000 sequencer. Quality control for concentration and library size distribution was performed using an Agilent Bioanalyzer DNA 1000 chip and Qubit fluorometry (Invitrogen, Carlsbad, CA). Sequence alignment of reads and determination of normalized gene counts were performed using the MAP-RSeq (v.1.2.1) workflow, utilizing TopHat 2.0.6 (Kim et al. 2013), and HTSeq (Anders et al. 2015). Normalized read counts were expressed as reads per kilobasepair per million mapped reads (RPKM). For muscle samples, raw read counts were obtained from the GEO database (accession#: GSE60591) and these counts were subjected to the same bioinformatic process as the samples obtained in this study.

2.3. Computational analysis and statistics

Normalized read counts generated from the RNA sequencing data were analyzed to assess differential gene expression between growth plate, articular cartilage, bone, and muscle specimens. Genes with an RPKM value > 0.3 in at least one tissue type were included in subsequent computational analyses. Discovery of differentially expressed genes (Physis vs. Bone/Cartilage/Muscle) was determined using the Two-stage linear step-up procedure of Benjamini, Krieger and Yekutieli with Q = 5% in GraphPad Prism version 7.03 for Windows. A volcano plot was generated using R Version 3.4.0 (Team 2017). Venn Diagrams were generated using InteractiVenn online tool (Heberle et al. 2015). Functional annotation clustering of differentially expressed genes was performed using DAVID Bioinformatics Resources 6.8 database (DAVID 6.8) (Shannon et al. 2003, da Huang et al., 2009). GO Term networks were created using the ClueGO plug-in within the Cytoscape software environment (Shannon et al., 2003, Bindea et al. 2009). Hierarchical clustering was performed using Morpheus matrix visualization and analysis software after a Log2 adjustment was made for each gene row (Broad Institute). Protein-protein interaction networks were generated using STRING Database version 10.5 (Szklarczyk et al. 2015; Szklarczyk et al. 2017).

2.4. Histological analysis

All tissues were fixed overnight in 10% neutral buffered formalin. Then, samples were washed and dehydrated in graded series of ethanol (70% to 100%) and processed with xylene (50% to 100%) prior to paraffin embedding. Paraffin blocks were cut into consecutive sections of 5 μm thickness using a microtome and placed onto charged microscope glass slides for histological staining. Following deparaffinization, sections were stained for proteoglycan content using 0.125% safranin-O

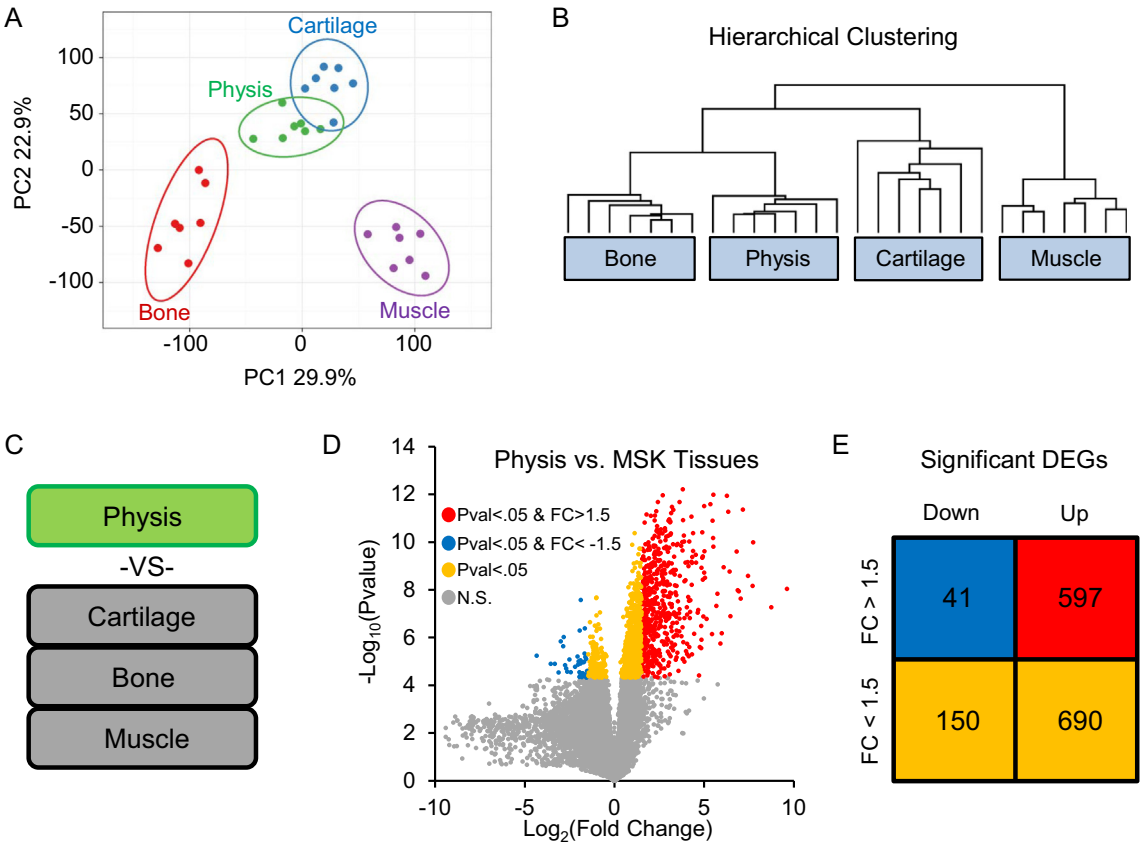

Fig. 1. Comparative analysis of mRNA expression in physis, bone, articular cartilage, and muscle. RNA sequencing was performed on musculoskeletal tissue samples (n = 7 for each tissue). Unbiased principal component analysis (PCA) (A) and hierarchical clustering (B) were performed using RPKM values for all genes with RPKM > 0.3 in at least one tissue. Comparative analysis of expression data was conducted as indicated (C). Volcano plot depicting Log_2(fold change) vs. $-Log_{10}$(Pvalue) calculated for each gene upon comparative analysis (D). Number of significant differentially expressed genes (DEGs) in physis compared to the other three tissues (E).

counterstained with Weigert's iron hematoxylin and 0.4% fast green staining (all from Sigma-Aldrich).

The presence of Frizzled 10 (FZD10) and collagen type IX (COL9A1) were determined by immunohistochemistry (IHC). In brief, after removal of paraffin and rehydration, sections were washed with distilled water. Antigen retrieval was performed as follows. For collagen type IX, the sections were subject to 1 mg/mL pronase (Sigma-Aldrich) for 30 min at 37 °C, followed by 10 mg/mL hyaluronidase (Sigma-Aldrich) incubation for 30 min at 37 °C. For FZD10, the sections were exposed to 10 mg/mL pepsin (Roche) for 20 min at 37 °C in a humidified chamber followed by 10 min incubation at room temperature. Subsequently, the sections were blocked using a 5% bovine serum albumin (BSA, Sigma-Aldrich) in PBS solution for 1 h, followed by an overnight incubation at 4 °C with a primary antibody against human type IX collagen (rabbit anti-human type IX collagen, ab134568, 1:100 dilution in PBS-BSA-5%; Abcam), human FZD10 (rabbit anti-human FZD10, ab150564, 1:150 dilution in PBS-BSA-5%; Abcam) and human IgG (rabbit anti-human IgG, PP64B, 1:1000 dilution in PBS-BSA-5%; Millipore). After washing, slides were sequentially incubated with a horseradish peroxidase-conjugated anti-rabbit secondary antibody (1:100 dilution in PBS-BSA-5%) for 60 min at room temperature and were then treated with 3,3′-diaminobenzidine (DAB) enhanced liquid substrate system for IHC (Sigma-Aldrich) diluted 1:1 with TBS (Tris-buffered saline) for 10 min until color development. The sections were counterstained with Harris's hematoxylin for 30 s. Immunoreactivity was visualized using a ZEISS Axio inverted light microscope.

3. Results

3.1. Comparative analysis of mRNA expression in physis, bone, articular cartilage, and muscle

RNA sequencing was performed using mRNA isolated from human physis, articular cartilage, bone, and muscle tissue samples (n = 7 for each tissue). To gain an understanding of how the transcriptome of these different tissue types compared across all samples and groups, we conducted unbiased principal component analysis (PCA) (Fig. 1A) and hierarchical clustering (Fig. 1B). We note distinct clustering of each tissue type in both the PCA and hierarchical clustering. It is important to note the slight overlap between the physis and articular cartilage tissues in the PCA. To further investigate the specific genes driving this distinct clustering in the physis, we compared physis tissue to the three other musculoskeletal tissues (Fig. 1C). In doing so, we generated gene sets demonstrating statistically significant alterations in expression levels within the physis (Fig. 1D). Specifically, 597 genes were significantly upregulated (Supplemental Table 2), and 41 genes were significantly downregulated (Supplemental Table 3) in the physis (Fig. 1E).

3.2. Functional analysis of physis-specific genes

With the 597 upregulated genes identified in the comparative analysis (Supplemental Table 2), we performed gene ontology (GO) analysis using ClueGO within Cytoscape (Shannon et al., 2003). This analysis revealed enrichment of GO Biological Process terms involved in skeletal system development including endochondral bone

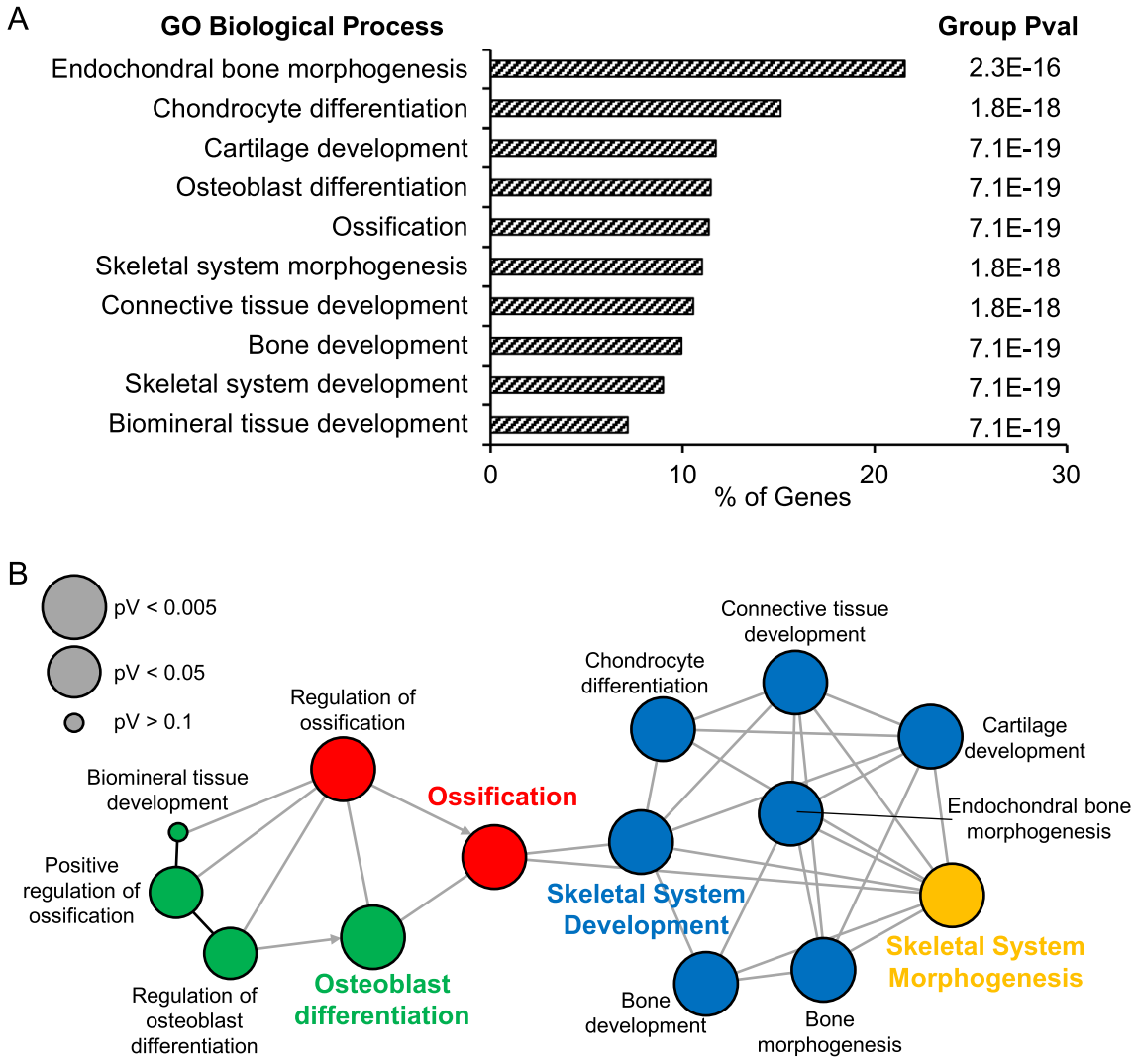

Fig. 2. Functional analysis of physis-specific genes. Gene Ontology-Biological Process (GO-BP) terms enriched upon ClueGo network analysis of the 597 upregulated physis-specific genes (A) form an interconnected network (B).

morphogenesis, chondrocyte and osteoblast differentiation, cartilage development, and skeletal system development (Fig. 2A). Subsequent network analysis shows interplay between GO Biological Process terms skeletal system development and morphogenesis, as well as ossification and chondrocyte and cartilage (Fig. 2B).

3.3. Physis-specific secretome involves distinct collagen networks

To corroborate our findings generated in the ClueGo analysis, we performed a second functional annotation clustering using DAVID 6.8. As anticipated, we observed enrichment for GO terms involved in musculoskeletal development including Glycoprotein, Extracellular Matrix, and Collagen (Fig. 3A). We also note significant enrichment of the clinically-relevant terms Dwarfism and Ehlers-Danlos Syndrome (EDS). Of note, the molecular terms “Signal”, “Secreted”, and “Receptor” were also significantly enriched. To further investigate this finding, we performed hierarchical clustering using the expression values for the genes associated with the “Secreted” keyword (n = 146, Supplemental Table 4) (Fig. 3B). Physis tissue displays a distinct expression pattern for “Secreted” genes, yet we note clusters of genes demonstrating similar expression patterns within cartilage and bone, and a close clustering of physis tissue to the articular cartilage samples. To better understand the functional role of these secreted genes, we performed ClueGo analysis using this same gene set (Supplemental Table 4) and observed significant enrichment of nodes centered around collagen metabolism and fibril organization as well as cellular and extracellular organization (Fig. 3C).

To investigate these interaction networks at the protein level, we conducted STRING analysis using the “Secreted” gene set. We observe a dense protein-protein interaction network involving the Collagens, ADAMTSs, and Matrilins (Fig. 3D). Hierarchical clustering analysis using the mRNA expression values for the genes involved in this protein-protein interaction network demonstrated a distinct expression pattern in Physis (Fig. 3E). Physis tissues cluster most closely with articular cartilage, while bone and muscle form a distinct clade. This clustering is to be expected as the physis contains chondrocytes which are also found in articular cartilage. The expression patterns of secreted genes that define the physis tissue cluster are shared to different degrees between articular cartilage and bone, but clearly not with skeletal muscle. We further focused our analysis on the most highly expressed collagen subtypes (RPKM > 100) in physis (Fig. 3F), and compared their average expression to that of the other three tissues (Fig. 3G). In the physis, there is elevated expression of cartilage-specific COL2A1, the ubiquitous bone and connective tissue-related COL1A1, as well as COL9A1 which was previously associated with the physis (Keene et al. 1995). Interestingly, we observed elevated levels of COL6A1, COL14A1, and COL16A1 in physis when compared to the other three tissues. ANOVA and subsequent Tukey's multiple comparisons test confirmed

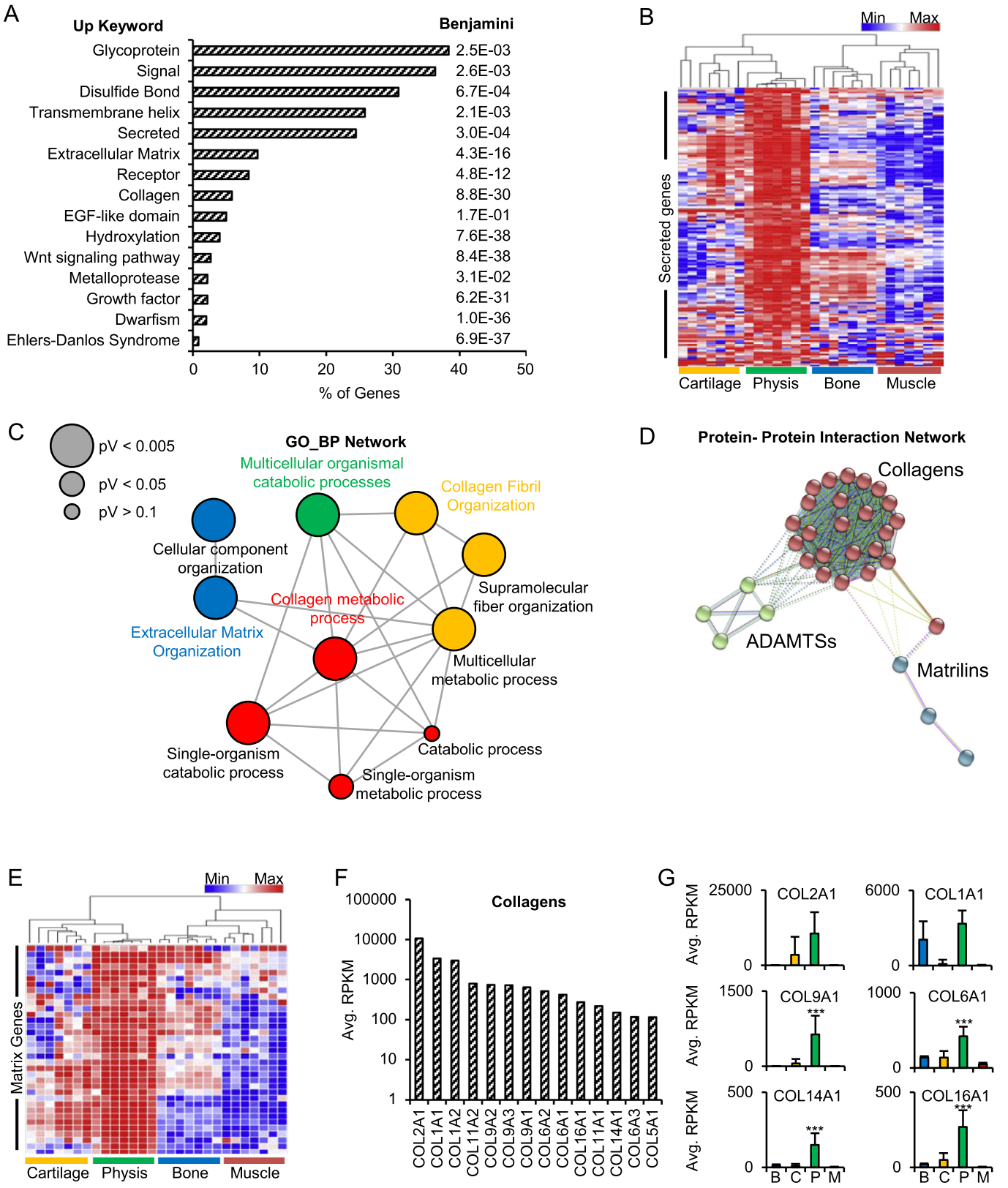

Fig. 3. Physis-specific secretome involves distinct collagen networks. Functional annotation clustering of the 597 upregulated physis-specific genes using DAVID 6.8 (A). Hierarchical clustering of musculoskeletal tissues based on RPKM values for genes within the "Secreted" Keyword identified in the DAVID analysis (B). GO-BP term network analysis (C) and STRING protein-protein interaction network analysis (D) performed using the gene list derived from the "Secreted" Keyword. Hierarchical clustering of musculoskeletal tissues based on RPKM values for extracellular matrix genes identified in the STRING analysis (E). Average RPKM value in physis tissue (n = 7) for all collagen genes highly expressed (RPKM > 100) in the physis (F). Average RPKM values for indicated collagens in bone (blue), cartilage (yellow), physis (green), and muscle (red) tissues (G). Statistical significance of physis compared to the other three tissues is indicated (*$p < 0.05$, **$p < 0.01$, ***$p < 0.001$). (For interpretation of the references to color in this figure legend, the reader is referred to the web version of this article.)

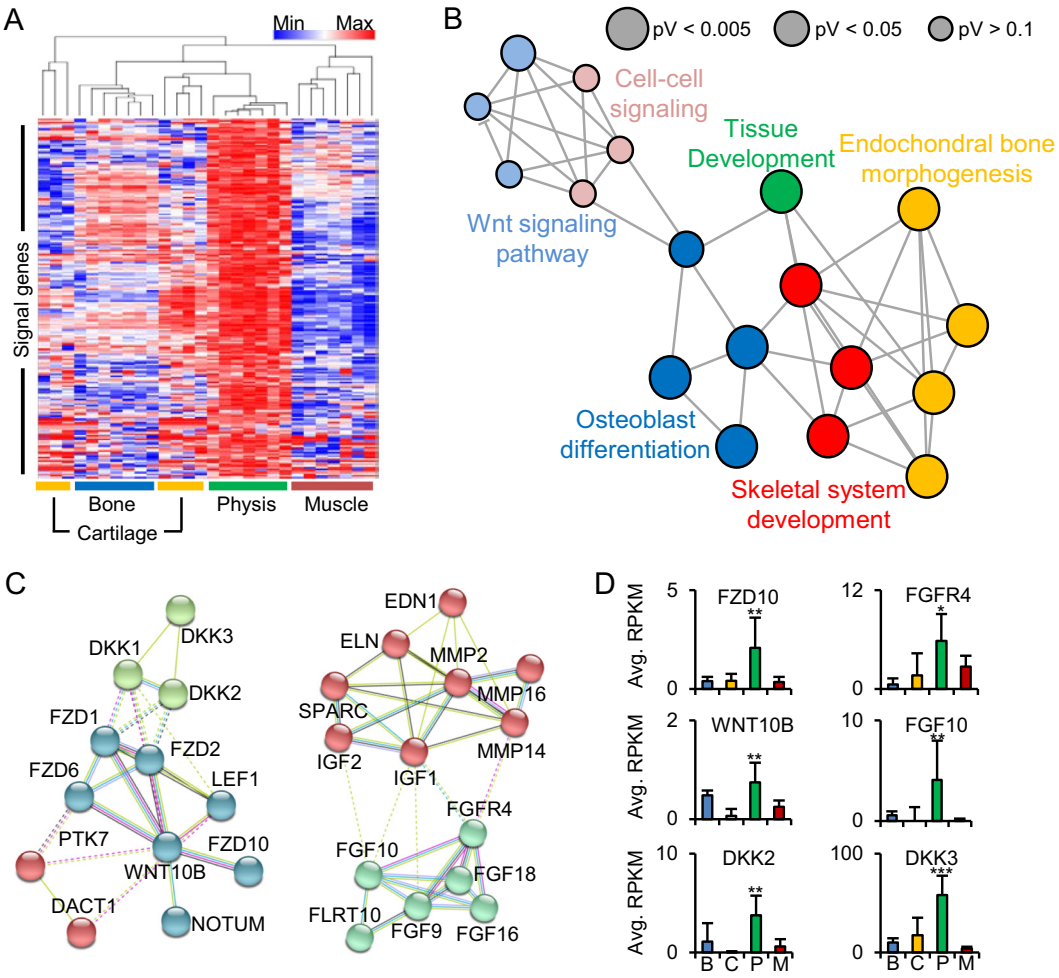

Fig. 4. Distinct signaling networks identified within the physis. Using the gene list associated with the enriched "Signal" Keyword (Fig. 3A), we performed hierarchical clustering of musculoskeletal tissues based on RPKM values (A), CluGO GO-BP network analysis (B), and STRING protein-protein interaction network analysis (C). Average RPKM values for identified genes in bone (blue), cartilage (yellow), physis (green), and muscle (red) tissues (D). Statistical significance of physis compared to the other three tissues is indicated (*$P < 0.05$, **$P < 0.01$, ***$P < 0.001$). (For interpretation of the references to color in this figure legend, the reader is referred to the web version of this article.)

that the expression of these collagens was significantly elevated in physis when compared to the combined average expression in the other three musculoskeletal tissues ($p < 0.0001$).

3.4. Distinct signaling networks are present within the physis

Similar to our analysis involving the "Secreted" genes, we examined genes within the "Signaling" keyword (n = 217, Supplemental Table 5) to elucidate signaling pathways unique to the physis. Upon hierarchal clustering analysis, the physis demonstrated distinct expression of "Signaling" genes (Fig. 4A). ClueGO analysis of the signaling genes enriched in the physis revealed clusters including Wnt signaling pathway, cell-cell signaling, tissue development, endochondral bone morphogenesis, and skeletal system development (Fig. 4B). STRING analysis demonstrated protein-protein interactions involving the WNT signaling (WNT10B, FZD1, FZD2, DKK1) and FGF signaling (FGF10, FGF18, FGFR4) pathways (Fig. 4C). We note that several genes involved in these signaling pathways demonstrate increased physis-specific expression when compared to bone, articular cartilage, and muscle (Fig. 4D). ANOVA and subsequent Tukey's multiple comparisons test confirmed that the expression of these signaling molecules was significantly elevated in physis when compared to the other three tissues.

3.5. Histological analysis of physis-specific proteins

To validate our findings from the differential gene expression analysis, we performed additional histological assays for the newly characterized growth plate-related genes using immunohistochemistry (IHC). This technique allows for confirmation that these highly expressed mRNAs are translated into protein and also provides a better understanding of their specific location within the physis. IHC experiments were performed in whole metatarsals derived from pediatric patients (Fig. 5C) which retains the in situ integrity of the growth plate. Safranin-O and Fast Green staining highlights the distinct regions of bone (blue) and cartilage (red) within the tissue sections (Fig. 5A). We conducted IHC for COL9A1 (Fig. 5B top) and FZD10 (Fig. 5B middle) because these proteins are encoded by genes that are among the most differentially expressed mRNAs within physeal tissue. For both proteins, we note localization to the hypertrophic and ossification zones of the physis.

3.6. Molecular analysis reveals novel physis-specific markers and signaling proteins

Together, our analyses reveal differential expression patterns in the growth plate compared to other musculoskeletal tissues. The physis serves as a developmental transition zone between cartilage and bone,

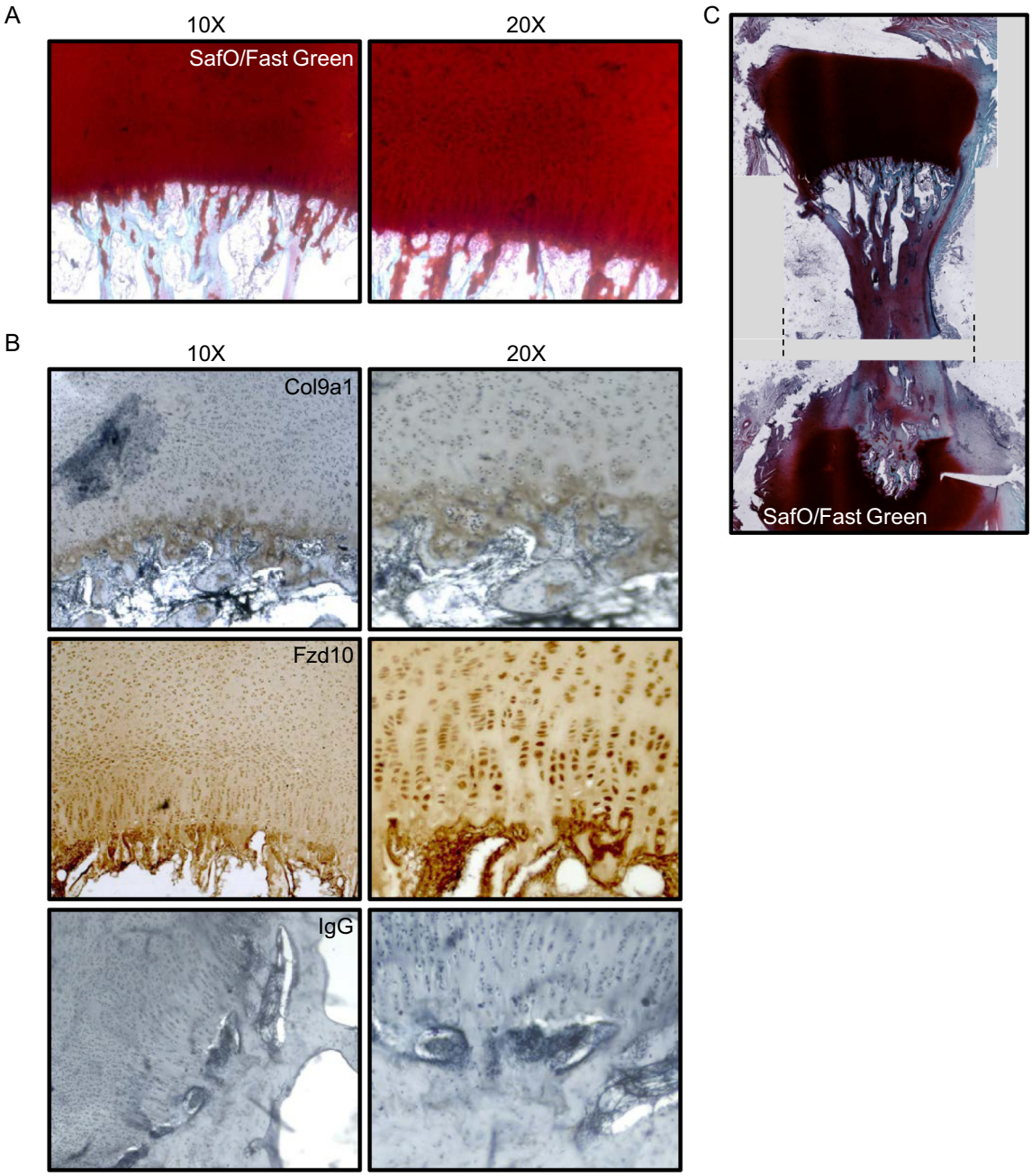

Fig. 5. Immunohistochemical analysis of newly identified physis-specific proteins. Safranin-O and Fast Green Staining (A) and immunohistochemistry with indicated antibodies (B) performed on sections of a human infant metatarsal (C)·Tissue high in proteoglycan content (cartilage) appears red after Safranin-O staining and collagen rich regions appear blue after Fast Green staining. Transition regions between bone and cartilage appear orange. Tissue sections positive for the protein of interest appear dark brown after completion of the IHC protocol. (For interpretation of the references to color in this figure legend, the reader is referred to the web version of this article.)

and therefore has similarities to both tissues. However, our study has revealed novel structural (collagen VI, XIV, and XVI) and signaling (FZD10, FGFR4, and FGF10) markers specific to growth plate which may be used for targeted therapies and interventions (Fig. 6).

4. Discussion

Current treatment strategies for physis disorders involve surgical management with guided growth, epiphyseodesis, physeal bar resection, osteotomy, or fusion surgery. There is a critical need for biological therapy to guide regeneration of physeal tissue or accelerate/decelerate limb growth. Previous work has demonstrated the utility of sequencing technologies in identifying key players in growth plate development (Nilsson et al. 2007; Emons et al. 2011; Leijten et al. 2012). Therefore, we reasoned that the high resolution molecular analysis presented in this study would provide a foundation for identifying cellular pathways and networks that could be pharmacologically targeted. Upon comparing physis tissue to articular cartilage, bone, and muscle, our study identified physis-specific gene sets exhibiting significant differential expression. Specifically, there are molecular similarities between physis, articular cartilage and bone. Physis tissue tends to cluster more closely with articular cartilage than bone, and displays gene expression patterns very distinct from muscle tissue. The similarity between physis and cartilage tissue is expected, because both contain chondrocytes that

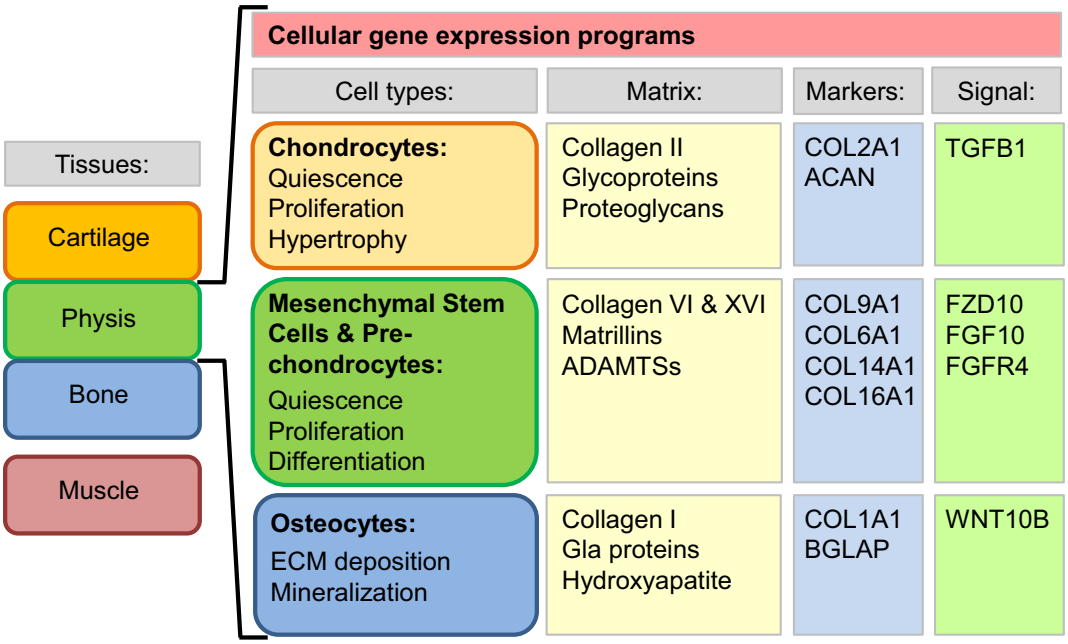

Fig. 6. Molecular analysis reveals novel physis-specific markers and signaling proteins. Summary diagram listing cell types, ECM proteins, and signaling molecules present within the physis.

contribute to similarities in gene expression patterns. Nonetheless, the physis represents a distinct anatomical structure, and our findings in the present study reflect this distinction at the molecular level.

Functional annotation analysis of the physis-specific gene set yielded enrichment of expected GO terms involving skeletal development and bone formation, and also identified potential physis-specific secretory and signaling pathways. The latter are of particular interest, because they represent a potential means of identifying growth plate specific proteins that could serve as pharmacological targets. Clusters of extracellular matrix proteins, particularly collagens, also emerged from our analyses, including mRNAs for several collagen subtypes (e.g., COL2A1, COL6A1, COL9A1, COL9A2, COL9A3, and COL11A2) that are known to be expressed in the physis (Hausler et al. 2002; Brachvogel et al. 2013). A new finding is the observed expression of mRNAs for COL16A1 and COL14A1 specifically in the physis. These findings suggest a physis-specific subset of collagens may form the extracellular matrix within the physis. Our study also revealed that several cartilage-associated non-collagenous extracellular matrix proteins are robustly expressed in the physis (e.g., matrillins). Remarkably, matrillin-3 (MATN3) collagen IX isoforms (COL9A1, COL9A2, COL9A3) have been linked to multiple epiphyseal dysplasias, a syndrome characterized by degenerative arthritis and disorganized endochondral ossification of the epiphysis (Jackson et al. 2012). Collagen VI is commonly found in a variety of tissues associated with the basement membrane, and mutations have been associated with Bethlem myopathy and Ullrich congenital muscular dystrophy (Bonnemann 2011). In articular cartilage, collagen VI microfibrils protect chondrocytes from compressive forces and are located primarily in the pericellular matrix (Owida et al. 2017). Interestingly, collagen VI knockout mice have only mild myopathy and muscle fibrosis with normal life expectancy (Pan et al. 2014). Collagens XIV and XVI have previously been reported in fetal bovine articular cartilage (Watt et al. 1992), and have been implicated as a biomarker of osteoarthritis (Agarwal et al. 2012).

Although collagen proteins are not druggable enzymes, insight into the specific location of different collagen subtypes within the physis may allow for a better understanding of the growth inhibition and angular deformities observed in pediatric patients with genetic alterations in collagen encoding genes. This information may also allow for a more targeted approach for surgical intervention (i.e. placement of hardware for guided growth) and/or inform scaffold design for reconstruction of traumatic injuries to the growth plate. Our analysis provides an example of this concept in identifying the localization of collagen IX (encoded by COL9A1) to the hypertrophic and ossification zone of the physis. The localization of collagen IX to this region suggests an important structural role in supporting extracellular matrix deposition during columnar formation of hypertrophic chondrocytes before ossification.

Similar to our findings from the analysis of secreted genes, our study established a unique physis-specific signature of genes encoding secreted proteins involved in cell signaling (e.g., WNT10B, FZD1, FZD2, DKK1). WNT signaling is known to be involved in limb growth and cartilage development (Ma et al. 2013; Zhong et al. 2016), which is consistent with the observed upregulation of several members of the WNT signaling pathway in the growth plate. Our histological analysis of FZD10 revealed localization to the hypertrophic region of the physis suggesting this signaling molecule may drive chondrocyte hypertrophy and maturation in the. WNT and other signaling pathways may provide pharmacological targets for growth plate therapeutics and regeneration strategies.

The studies presented here establish the transcriptomic profiles of human physis tissues in comparison with cartilage, bone and muscle tissues. One limitation of our work is that RNA-seq analyses were performed on whole tissues, which may include different anatomical zones, blood vessels and/or infiltrating cell types (e.g. bone, connective tissues, blood). Hence, some of the expression signatures we documented may derive from these other biological sources. For example, all tissues we analyzed exhibited expression of hemoglobin β (HBB) mRNA which indicates that RNAs from erythroid cells were included in the RNA isolation procedure. In addition, we detected moderate levels of expression of COL1A1 in the growth plate, perhaps reflecting the presence of adjacent bone tissues from the zone of ossification that were hard to dissect during surgical isolation of specimens from pediatric patients undergoing limb ablation. Furthermore, our analysis of the growth plate did not discriminate between proliferative, resting and hypertrophic zones of the growth plate. Limitations related to exact anatomical location will be addressed by laser capture microdissection which necessitates fixation of embedded tissues, unlike our current surgical specimens. Regardless, the transcriptome profiles described

here have proven to be informative and permit generation of viable hypotheses that will enable us to investigate strategies for controlling the growth and differentiation of cartilaginous cells in the human physis.

5. Conclusion

Advancement of knowledge in physis research is crucial to fostering tissue engineering and drug delivery strategies to restore or regenerate damaged cartilaginous structures and treat growth plate-associated diseases. Utilizing our large dataset of clinical specimens and computational analysis, we have identified gene regulatory networks in physis tissue that are associated with regulation of extracellular matrix synthesis and limb growth. Results from these studies can be used to optimize and validate tissue engineering strategies and develop novel pharmacologic approaches for the treatment of diseases affecting the growth plate. Together, our findings have validated the concept that physis is a distinct tissue characterized by a distinct molecular signature. A better understanding of the signal transduction mechanisms in the human growth plate is critical to avoid complex surgical reconstructions and to promote development of therapeutics aimed at treating pediatric limb deformities and growth plate disorders.

Supplementary data to this article can be found online at https://doi.org/10.1016/j.gene.2018.05.034.

Acknowledgments

We thank the members or our laboratories and institutional colleagues for their enthusiastic support throughout these studies. We are especially grateful to Tad Mabry, Thomas Shives, Amy McIntosh, Anthony Stans, Peter Amadio, Michael Nicoson, and William Shaughnessy for their help in procuring patient samples as well as Vickie Treder, Asha Nair, Eric Lewallen and Chenghao Zhang for assistance with tissue processing, RNA isolation procedures and/or bioinformatics. We would also like to thank Janet Denbeigh, Emily Camilleri, Jennifer Grauberger, Mario Hevesi, and Carlo Paggi for stimulating discussions. In addition, we thank William and Karen Eby for their charitable contributions that enable us to pursue this work.

Declaration of conflicting interests

Todd A. Milbrandt is on the POSNA board of Directors, a Viking Scientific-Stock holder, an Orthopediatrics-consultant, and a Broadwater-CME course Director. A. Noelle Larson- Research funding from Orthopediatrics and K2M.

Author contributions

CP, AJvW, and ANL designed the study. CP, CG-G, DG-G performed the biological and computational studies. CP, CG-G. AD, TAM, DBFS, AJK, MK, GBF, DE, SMR, AJvW, and ANL provided interpretation of the results. CP, ANL and AJvW prepared the manuscript with comments from all authors.

Funding

This publication was made possible by CTSA Grant Number UL1 TR000135 from the National Center for Advancing Translational Sciences (NCATS), a component of the National Institutes of Health (NIH). Its contents are solely the responsibility of the authors and do not necessarily represent the official view of NIH.

The work was supported by a grant from the National Institute of Arthritis and Musculoskeletal and Skin Diseases (R03 AR066342 to ANL; R01 AR069049 to AvW), as well as funding from the Mayo Clinic Center of Regenerative Medicine. We thank William and Karen Eby for generous philanthropic support.

References

Agarwal, P., Zwolanek, D., Keene, D.R., Schulz, J.N., Blumbach, K., Heinegard, D., Zaucke, F., Paulsson, M., Krieg, T., Koch, M., Eckes, B., 2012. Collagen XII and XIV, new partners of cartilage oligomeric matrix protein in the skin extracellular matrix suprastructure. J. Biol. Chem. 287 (27), 22549–22559.

Anders, S., Pyl, P.T., Huber, W., 2015. HTSeq—a Python framework to work with high-throughput sequencing data. Bioinformatics 31 (2), 166–169.

Andrade, A.C., Lui, J.C., Nilsson, O., 2010. Temporal and spatial expression of a growth-regulated network of imprinted genes in growth plate. Pediatr. Nephrol. 25 (4), 617–623.

Bindea, G., Mlecnik, B., Hackl, H., Charoentong, P., Tosolini, M., Kirilovsky, A., Fridman, W.H., Pages, F., Trajanoski, Z., Galon, J., 2009. ClueGO: a Cytoscape plug-in to decipher functionally grouped gene ontology and pathway annotation networks. Bioinformatics 25 (8), 1091–1093.

Black, S.R., Kwon, M.S., Cherkashin, A.M., Samchukov, M.L., Birch, J.G., Jo, C.H., 2015. Lengthening in congenital femoral deficiency: a comparison of circular external fixation and a motorized intramedullary nail. J. Bone Joint Surg. Am. 97 (17), 1432–1440.

Bonnemann, C.G., 2011. The collagen VI-related myopathies Ullrich congenital muscular dystrophy and Bethlem myopathy. Handb. Clin. Neurol. 101, 81–96.

Brachvogel, B., Zaucke, F., Dave, K., Norris, E.L., Stermann, J., Dayakli, M., Koch, M., Gorman, J.J., Bateman, J.F., Wilson, R., 2013. Comparative proteomic analysis of normal and collagen IX null mouse cartilage reveals altered extracellular matrix composition and novel components of the collagen IX interactome. J. Biol. Chem. 288 (19), 13481–13492.

Clark, A., Hilt, J.Z., Milbrandt, T.A., Puleo, D.A., 2015. Treating proximal tibial growth plate injuries using poly(lactic-co-glycolic acid) scaffolds. Bioresour. Open Access 4 (1), 65–74.

Dudakovic, A., Camilleri, E., Riester, S.M., Lewallen, E.A., Kvasha, S., Chen, X., Radel, D.J., Anderson, J.M., Nair, A.A., Evans, J.M., Krych, A.J., Smith, J., Deyle, D.R., Stein, J.L., Stein, G.S., Im, H.J., Cool, S.M., Westendorf, J.J., Kakar, S., Dietz, A.B., van Wijnen, A.J., 2014. High-resolution molecular validation of self-renewal and spontaneous differentiation in clinical-grade adipose-tissue derived human mesenchymal stem cells. J. Cell. Biochem. 115 (10), 1816–1828.

Emons, J., Dutilh, B.E., Decker, E., Pirzer, H., Sticht, C., Gretz, N., Rappold, G., Cameron, E.R., Neil, J.C., Stein, G.S., van Wijnen, A.J., Wit, J.M., Post, J.N., Karperien, M., 2011. Genome-wide screening in human growth plates during puberty in one patient suggests a role for RUNX2 in epiphyseal maturation. J. Endocrinol. 209 (2), 245–254.

Galeano-Garces, C., Camilleri, E.T., Riester, S.M., Dudakovic, A., Larson, D.R., Qu, W., Smith, J., Dietz, A.B., Im, H.J., Krych, A.J., Larson, A.N., Karperien, M., van Wijnen, A.J., 2017. Molecular validation of chondrogenic differentiation and hypoxia responsiveness of platelet-lysate expanded adipose tissue-derived human mesenchymal stromal cells. Cartilage 8 (3), 283–299.

Hantes, M.E., Malizos, K.N., Xenakis, T.A., Beris, A.E., Mavrodontidis, A.N., Soucacos, P.N., 2001. Complications in limb-lengthening procedures: a review of 49 cases. Am. J. Orthop. (Belle Mead N.J.) 30 (6), 479–483.

Hausler, G., Helmreich, M., Marlovits, S., Egerbacher, M., 2002. Integrins and extracellular matrix proteins in the human childhood and adolescent growth plate. Calcif. Tissue Int. 71 (3), 212–218.

Heberle, H., Meirelles, G.V., da Silva, F.R., Telles, G.P., Minghim, R., 2015. InteractiVenn: a web-based tool for the analysis of sets through Venn diagrams. BMC Bioinf. 16, 169.

Huang da, W., Sherman, B.T., Lempicki, R.A., 2009. Systematic and integrative analysis of large gene lists using DAVID bioinformatics resources. Nat. Protoc. 4 (1), 44–57.

Jackson, G.C., Mittaz-Crettol, L., Taylor, J.A., Mortier, G.R., Spranger, J., Zabel, B., Le Merrer, M., Cormier-Daire, V., Hall, C.M., Offiah, A., Wright, M.J., Savarirayan, R., Nishimura, G., Ramsden, S.C., Elles, R., Bonafe, L., Superti-Furga, A., Unger, S., Zankl, A., Briggs, M.D., 2012. Pseudoachondroplasia and multiple epiphyseal dysplasia: a 7-year comprehensive analysis of the known disease genes identify novel and recurrent mutations and provides an accurate assessment of their relative contribution. Hum. Mutat. 33 (1), 144–157.

Kalari, K.R., Nair, A.A., Bhavsar, J.D., O'Brien, D.R., Davila, J.I., Bockol, M.A., Nie, J., Tang, X., Baheti, S., Doughty, J.B., Middha, S., Sicotte, H., Thompson, A.E., Asmann, Y.W., Kocher, J.P., 2014. MAP-RSeq: Mayo analysis pipeline for RNA sequencing. BMC Bioinf. 15, 224.

Keene, D.R., Oxford, J.T., Morris, N.P., 1995. Ultrastructural localization of collagen types II, IX, and XI in the growth plate of human rib and fetal bovine epiphyseal cartilage: type XI collagen is restricted to thin fibrils. J. Histochem. Cytochem. 43 (10), 967–979.

Kim, D., Pertea, G., Trapnell, C., Pimentel, H., Kelley, R., Salzberg, S.L., 2013. TopHat2: accurate alignment of transcriptomes in the presence of insertions, deletions and gene fusions. Genome Biol. 14 (4), R36.

Kronenberg, H.M., 2003. Developmental regulation of the growth plate. Nature 423 (6937), 332–336.

Launay, F., Younsi, R., Pithioux, M., Chabrand, P., Bollini, G., Jouve, J.L., 2013. Fracture following lower limb lengthening in children: a series of 58 patients. Orthop. Traumatol. Surg. Res. 99 (1), 72–79.

Leijten, J.C., Emons, J., Sticht, C., van Gool, S., Decker, E., Uitterlinden, A., Rappold, G., Hofman, A., Rivadeneira, F., Scherjon, S., Wit, J.M., van Meurs, J., van Blitterswijk, C.A., Karperien, M., 2012. Gremlin 1, frizzled-related protein, and Dkk-1 are key regulators of human articular cartilage homeostasis. Arthritis Rheum. 64 (10), 3302–3312.

Lewallen, E.A., Bonin, C.A., Li, X., Smith, J., Karperien, M., Larson, A.N., Lewallen, D.G., Cool, S.M., Westendorf, J.J., Krych, A.J., Leontovich, A.A., Im, H.J., van Wijnen, A.J., 2016. The synovial microenvironment of osteoarthritic joints alters RNA-seq

expression profiles of human primary articular chondrocytes. Gene 591 (2), 456–464.
Lin, Y., Lewallen, E.A., Camilleri, E.T., Bonin, C.A., Jones, D.L., Dudakovic, A., Galeano-Garces, C., Wang, W., Karperien, M.J., Larson, A.N., Dahm, D.L., Stuart, M.J., Levy, B.A., Smith, J., Ryssman, D.B., Westendorf, J.J., Im, H.J., van Wijnen, A.J., Riester, S.M., Krych, A.J., 2016. RNA-seq analysis of clinical-grade osteochondral allografts reveals activation of early response genes. J. Orthop. Res. 34 (11), 1950–1959.
Lindholm, M.E., Huss, M., Solnestam, B.W., Kjellqvist, S., Lundeberg, J., Sundberg, C.J., 2014. The human skeletal muscle transcriptome: sex differences, alternative splicing, and tissue homogeneity assessed with RNA sequencing. FASEB J. 28 (10), 4571–4581.
Lui, J.C., Andrade, A.C., Forcinito, P., Hegde, A., Chen, W., Baron, J., Nilsson, O., 2010. Spatial and temporal regulation of gene expression in the mammalian growth plate. Bone 46 (5), 1380–1390.
Ma, B., Landman, E.B., Miclea, R.L., Wit, J.M., Robanus-Maandag, E.C., Post, J.N., Karperien, M., 2013. WNT signaling and cartilage: of mice and men. Calcif. Tissue Int. 92 (5), 399–411.
Marino, R., 2011. Growth plate biology: new insights. Curr. Opin. Endocrinol. Diabetes Obes. 18 (1), 9–13.
Myllyharju, J., 2014. Extracellular matrix and developing growth plate. Curr. Osteoporos. Rep. 12 (4), 439–445.
Nilsson, O., Parker, E.A., Hegde, A., Chau, M., Barnes, K.M., Baron, J., 2007. Gradients in bone morphogenetic protein-related gene expression across the growth plate. J. Endocrinol. 193 (1), 75–84.
Owida, H.A., De Las Heras Ruiz, T., Dhillon, A., Yang, Y., Kuiper, N.J., 2017. Co-culture of chondrons and mesenchymal stromal cells reduces the loss of collagen VI and improves extracellular matrix production. Histochem. Cell Biol. 148 (6), 625–638.
Pan, T.C., Zhang, R.Z., Arita, M., Bogdanovich, S., Adams, S.M., Gara, S.K., Wagener, R., Khurana, T.S., Birk, D.E., Chu, M.L., 2014. A mouse model for dominant collagen VI disorders: heterozygous deletion of Col6a3 Exon 16. J. Biol. Chem. 289 (15), 10293–10307.
Riester, S.M., Lin, Y., Wang, W., Cong, L., Mohamed Ali, A.M., Peck, S.H., Smith, L.J., Currier, B.L., Clark, M., Huddleston, P., Krauss, W., Yaszemski, M.J., Morrey, M.E., Abdel, M.P., Bydon, M., Qu, W., Larson, A.N., van Wijnen, A.J., Nassr, A., 2017. RNA sequencing identifies gene regulatory networks controlling extracellular matrix synthesis in intervertebral disk tissues. J. Orthop. Res. http://dx.doi.org/10.1002/jor.23834. [Epub ahead of print].
Sanders, J.O., Khoury, J.G., Kishan, S., 2007. A technique for calculating limb length inequality and epiphyseodesis timing using the multiplier method and a spreadsheet. J. Child. Orthop. 1 (3), 217.
Shannon, P., Markiel, A., Ozier, O., Baliga, N.S., Wang, J.T., Ramage, D., Amin, N., Schwikowski, B., Ideker, T., 2003. Cytoscape: a software environment for integrated models of biomolecular interaction networks. Genome Res. 13 (11), 2498–2504.
Stevens, P.M., 2007. Guided growth for angular correction: a preliminary series using a tension band plate. J. Pediatr. Orthop. 27 (3), 253–259.
Szklarczyk, D., Franceschini, A., Wyder, S., Forslund, K., Heller, D., Huerta-Cepas, J., Simonovic, M., Roth, A., Santos, A., Tsafou, K.P., Kuhn, M., Bork, P., Jensen, L.J., von Mering, C., 2015. STRING v10: protein-protein interaction networks, integrated over the tree of life. Nucleic Acids Res. 43 (Database issue), D447–452.
Szklarczyk, D., Morris, J.H., Cook, H., Kuhn, M., Wyder, S., Simonovic, M., Santos, A., Doncheva, N.T., Roth, A., Bork, P., Jensen, L.J., von Mering, C., 2017. The STRING database in 2017: quality-controlled protein-protein association networks, made broadly accessible. Nucleic Acids Res. 45 (D1), D362–d368.
Team, R.C., 2017. R: A Language and Environment for Statistical Computing.
Watt, S.L., Lunstrum, G.P., McDonough, A.M., Keene, D.R., Burgeson, R.E., Morris, N.P., 1992. Characterization of collagen types XII and XIV from fetal bovine cartilage. J. Biol. Chem. 267 (28), 20093–20099.
Zhong, L., Huang, X., Rodrigues, E.D., Leijten, J.C., Verrips, T., El Khattabi, M., Karperien, M., Post, J.N., 2016. Endogenous DKK1 and FRZB regulate chondrogenesis and hypertrophy in three-dimensional cultures of human chondrocytes and human mesenchymal stem cells. Stem Cells Dev. 25 (23), 1808–1817.